Bacterial rhamnolipids and their 3-hydroxyalkanoate precursors activate Arabidopsis innate immunity through two independent mechanisms

Romain Schellenberger, Jérôme Crouzet, Arvin Nickzad, Lin-Jie Shu, Alexander Kutschera, Tim Gerster, Nicolas Borie, Corinna Dawid, Maude Cloutier, Sandra Villaume, et al.

Bacterial rhamnolipids and their 3-hydroxyalkanoate precursors activate *Arabidopsis* innate immunity through two independent mechanisms

Romain Schellenberger[a,1], Jérôme Crouzet[a,1], Arvin Nickzad[b], Lin-Jie Shu[c], Alexander Kutschera[c], Tim Gerster[c], Nicolas Borie[d], Corinna Dawid[e], Maude Cloutier[b], Sandra Villaume[a], Sandrine Dhondt-Cordelier[a], Jane Hubert[d,2], Sylvain Cordelier[a], Florence Mazeyrat-Gourbeyre[a], Christian Schmid[e], Marc Ongena[f], Jean-Hugues Renault[d], Arnaud Haudrechy[d], Thomas Hofmann[e], Fabienne Baillieul[a], Christophe Clément[a], Cyril Zipfel[g,h], Charles Gauthier[b], Eric Déziel[b,3], Stefanie Ranf[c,3], and Stéphan Dorey[a,3]

[a]Université de Reims Champagne-Ardenne, Unité de Recherche Résistance Induite et Bioprotection des Plantes, Unité d'accueil 4707, Institut National de Recherche pour l'Agriculture, l'Alimentation et l'Environnement, Unité sous contrat 1488, Structure Fédérative de Recherche Condorcet, CNRS, Fédération de Recherche 3417, 51687 Reims, France; [b]Centre Armand-Frappier Santé Biotechnologie, Institut National de la Recherche Scientifique, Laval, QC H7V 1B7, Canada; [c]Phytopathology, School of Life Sciences Weihenstephan, Technical University of Munich, Freising-Weihenstephan 85354, Germany; [d]Université de Reims Champagne-Ardenne, CNRS, Institut de Chimie Moléculaire, Unité Mixte de Recherche 7312, Structure Fédérative de Recherche Condorcet, CNRS, Fédération de Recherche 3417, 51687 Reims, France; [e]Food Chemistry and Molecular Sensory Science, School of Life Sciences Weihenstephan, Technical University of Munich, Freising-Weihenstephan 85354, Germany; [f]Microbial Processes and Interactions Laboratory, Structure Fédérative de Recherche Condorcet, CNRS, Fédération de Recherche 3417, Gembloux Agro-Bio Tech, University of Liège, Gembloux B-5030, Belgium; [g]The Sainsbury Laboratory, University of East Anglia, Norwich Research Park, Norwich NR4 7UH, United Kingdom; and [h]Institute of Plant and Microbial Biology, Zurich-Basel Plant Science Center, University of Zurich, CH-8008 Zurich, Switzerland

Edited by Xinnian Dong, Duke University, Durham, NC, and approved August 10, 2021 (received for review January 26, 2021)

Plant innate immunity is activated upon perception of invasion pattern molecules by plant cell-surface immune receptors. Several bacteria of the genera *Pseudomonas* and *Burkholderia* produce rhamnolipids (RLs) from L-rhamnose and (*R*)-3-hydroxyalkanoate precursors (HAAs). RL and HAA secretion is required to modulate bacterial surface motility, biofilm development, and thus successful colonization of hosts. Here, we show that the lipidic secretome from the opportunistic pathogen *Pseudomonas aeruginosa*, mainly comprising RLs and HAAs, stimulates *Arabidopsis* immunity. We demonstrate that HAAs are sensed by the bulb-type lectin receptor kinase LIPOOLIGOSACCHARIDE-SPECIFIC REDUCED ELICITATION/S-DOMAIN-1-29 (LORE/SD1-29), which also mediates medium-chain 3-hydroxy fatty acid (mc-3-OH-FA) perception, in the plant *Arabidopsis thaliana*. HAA sensing induces canonical immune signaling and local resistance to plant pathogenic *Pseudomonas* infection. By contrast, RLs trigger an atypical immune response and resistance to *Pseudomonas* infection independent of LORE. Thus, the glycosyl moieties of RLs, although abolishing sensing by LORE, do not impair their ability to trigger plant defense. Moreover, our results show that the immune response triggered by RLs is affected by the sphingolipid composition of the plasma membrane. In conclusion, RLs and their precursors released by bacteria can both be perceived by plants but through distinct mechanisms.

plant immunity | rhamnolipids | HAA | *Pseudomonas*

Plant innate immunity activation relies on detection of invasion pattern (IP) molecules that are perceived by plant cells (1, 2). Non–self-recognition IPs include essential components of whole classes of microorganisms, such as fragments of flagellin, peptidoglycans, mc-3-OH-FAs from bacteria or fragments of chitin, and β-glucans from fungi and oomycetes, respectively (3, 4). Apoplastic IPs are sensed by plant plasma membrane–localized receptor kinases (RKs) or receptor-like proteins (RLPs) that function as pattern recognition receptors (PRRs) (5, 6). Activation of the immune response requires the recruitment of regulatory receptor kinases and receptor-like cytoplasmic kinases (RLCKs) by PRRs (7). Early cellular immune signaling of pattern-triggered immunity (PTI) includes ion-flux changes at the plasma membrane, rise in cytosolic Ca^{2+} levels, production of extracellular reactive oxygen species (ROS), and activation of mitogen-activated protein kinases (MAPKs) and/or Ca^{2+}-dependent protein kinases (3, 8–10). Biosynthesis and mobilization of plant hormones, including salicylic acid, jasmonic acid, ethylene, abscisic acid and brassinosteroids, ultimately modulate plant resistance to phytopathogens (11–14).

Rhamnolipids (RLs) are extracellular amphiphilic metabolites produced by several bacteria, especially *Pseudomonas* and *Burkholderia* species (15–17). Acting as wetting agents, RLs are essential for bacterial surface dissemination called swarming

Significance

Activation of plant innate immunity relies on the perception of microorganisms through elicitors. Rhamnolipids and their precursor HAAs are exoproducts produced by bacteria. They are involved in bacterial surface dissemination and biofilm development. As these compounds are released in the extracellular milieu, they have the potential to be perceived by the plant immune system. Our work shows that both compounds independently activate plant immunity. We demonstrate that HAAs are perceived by the receptor protein kinase LORE. By contrast, rhamnolipids are not sensed by LORE but activate a noncanonical immune response influenced by the sphingolipid composition of the plant plasma membrane. Thus, plants can sense bacterial molecules as well as their direct precursors to trigger distinct immune responses.

Author contributions: J.C. and S.D. designed research; R.S., J.C., L.-J.S., A.K., T.G., S.V., and S.D.-C. performed research; R.S., J.C., S.C., F.M.-G., M.O., T.H., F.B., C.C., C.Z., E.D., S.R., and S.D. analyzed data; A.N., N.B., C.D., M.C., J.H., C.S., J.-H.R., A.H., C.G., and E.D. contributed new reagents/analytic tools; R.S., J.C., S.R., and S.D. wrote the paper; and M.O., T.H., F.B., C.C., C.Z., and E.D. contributed ideas and critically revised the manuscript.

Competing interest statement: Technical University of Munich has filed a patent application to inventors A.K., C.D., T.H., and S.R.

This article is a PNAS Direct Submission.

[1]R.S. and J.C. contributed equally to this work.

[2]Present address: NatExplore, 51140 Prouilly, France.

[3]To whom correspondence may be addressed. Email: stephan.dorey@univ-reims.fr, ranf@wzw.tum.de, or eric.deziel@iaf.inrs.ca.

This article contains supporting information online at https://www.pnas.org/lookup/suppl/doi:10.1073/pnas.2101366118/-/DCSupplemental.

Published September 24, 2021.

motility and for normal biofilm development (18–20). These glycolipids are produced from L-rhamnose and 3-(3-hydroxyalkanoyloxy)alkanoic acid (HAA) precursors (15, 21). HAAs are synthesized by dimerization of (*R*)-3-hydroxyalkanoyl-CoA in *Pseudomonas*, forming congeners through the RhlA enzyme (21). The opportunistic plant pathogen *Pseudomonas aeruginosa* and the phytopathogen *Pseudomonas syringae* produce extracellular HAAs (16, 22–24). In *P. syringae*, HAA synthesis is coordinately regulated with the late-stage flagellar gene encoding flagellin (22). HAA and RL production is finely tuned and modulates the behavior of swarming migrating bacterial cells by acting as self-produced negative and positive chemotactic-like stimuli (25). RLs contribute to the alteration of the bacterial outer membrane composition, by shedding flagellin from the flagella (26) and by releasing lipopolysaccharides (LPS), resulting in an increased hydrophobicity of the bacterial cell surface (27). In mammalian cells, RLs produced by *Burkholderia plantarii* exhibit endotoxin-like properties similar to LPS, leading to the production of proinflammatory cytokines in human mononuclear cells (28, 29). They also subvert the host innate immune response through manipulation of the human beta-defensin-2 expression (30). Moreover, RLs from *Burkholderia pseudomallei* induce interferon gamma (IFN-γ)–dependent host immune response in goat (31).

In plants, RLs induce defense responses and resistance to biotrophic and necrotrophic pathogens (32, 33). They also contribute to the biocontrol activity of the plant beneficial bacterium *P. aeruginosa* PNA1 against oomycetes (17). Recently, it was reported that the bulb-type lectin receptor kinase LIPOOLIGOSACCHARIDE-SPECIFIC REDUCED ELICITATION/S-DOMAIN-1-29 (LORE/SD1-29) mediates medium-chain 3-hydroxy fatty acid (mc-3-OH-FA) sensing in *Arabidopsis thaliana* (hereafter, *Arabidopsis*) and that bacterial compounds comprising mc-3-OH-acyl building blocks including LPS and RLs do not stimulate LORE-dependent responses (34).

Here, we show that the lipidic secretome produced by *P. aeruginosa* (RL secretome), mostly composed of RLs and HAAs, induces *Arabidopsis* immunity. HAAs are perceived through the RK LORE. We demonstrate that, albeit not being sensed by LORE, RLs trigger an immune response characterized by an atypical defense signature. Altogether, our results demonstrate that RLs and their precursors produced by *Pseudomonas* bacteria stimulate the plant immune response by two distinct mechanisms.

Results

RL Secretome from *Pseudomonas* Induces *Arabidopsis* Immune Responses Partially Mediated by LORE. *Pseudomonas* species, including opportunistic plant pathogenic or plant beneficial endophytic strains, release a mixture of RL congeners and HAA precursors, here collectively termed RL secretome (RLsec) (15, 25). High-performance liquid chromatography (HPLC)-tandem mass spectrometry (MS/MS) analyses of this RLsec from *P. aeruginosa* revealed the presence of mono-RLs and di-RLs at 50.9% and 44.9% of dry weight, respectively, and HAAs (3.8% of dry weight) (*SI Appendix*, Table S1 and Fig. S1). RLs comprising 10-carbon-long lipid tails, Rha-C_{10}-C_{10} (α-L-rhamnopyranosyl-β-hydroxydecanoyl-β-hydroxydecanoate) and Rha-Rha-C_{10}-C_{10} (α-L-rhamnopyranosyl-α-L-rhamnopyranosyl-β-hydroxydecanoyl-β-hydroxydecanoate), and C_{10}-C_{10} [(*R*)-3-(((*R*)-3-hydroxydecanoyl)oxy)decanoate] HAAs were the most abundant molecules in this lipidic secretome (37.6, 33.1, and 2.1%, respectively). Notably, low amounts of free mc-3-OH-FAs (0.4% total), such as 3-OH-C_8, 3-OH-C_{10}, and 3-OH-C_{12}, were also identified (*SI Appendix*, Table S1 and Fig. S1).

First, we monitored apoplastic ROS production triggered by RLsec in *Arabidopsis* (35). Wild-type (WT) plants challenged with RLsec displayed a transient extracellular ROS production, starting at 6 min and peaking at 15 min postelicitation (Fig. 1*A*). A robust ROS response was detected at concentrations of RLsec starting from 0.5 μg/mL (Fig. 1*B* and *SI Appendix*, Fig. S2). The ROS burst was dependent on the transmembrane NADPH oxidase RBOHD (36, 37) (Fig. 1*C* and *SI Appendix*, Fig. S3). RKs and RLPs mediate perception of IPs and early activation of PTI signaling (7). We monitored RLsec-triggered ROS production in *Arabidopsis* plants carrying loss-of-function mutations in genes encoding well-characterized RKs and RLPs *fls2*/*efr*-1 (38, 39), *bak1*-5, *bkk1*-1, *bak1*-5/*bkk1*-1 (40), *bik1*/*pbl1* (41), *cerk1*-2 (42), *sobir1*-12, *sobir1*-13 (43), *dorn1*-1 (44), and *lore*-5 (45). RLsec-induced production of ROS was only reduced in *lore*-5 (Fig. 1*C* and *SI Appendix*, Fig. S3). Some IPs, including LPS extracts and mc-3-OH-FAs, were reported to induce a late ROS production in

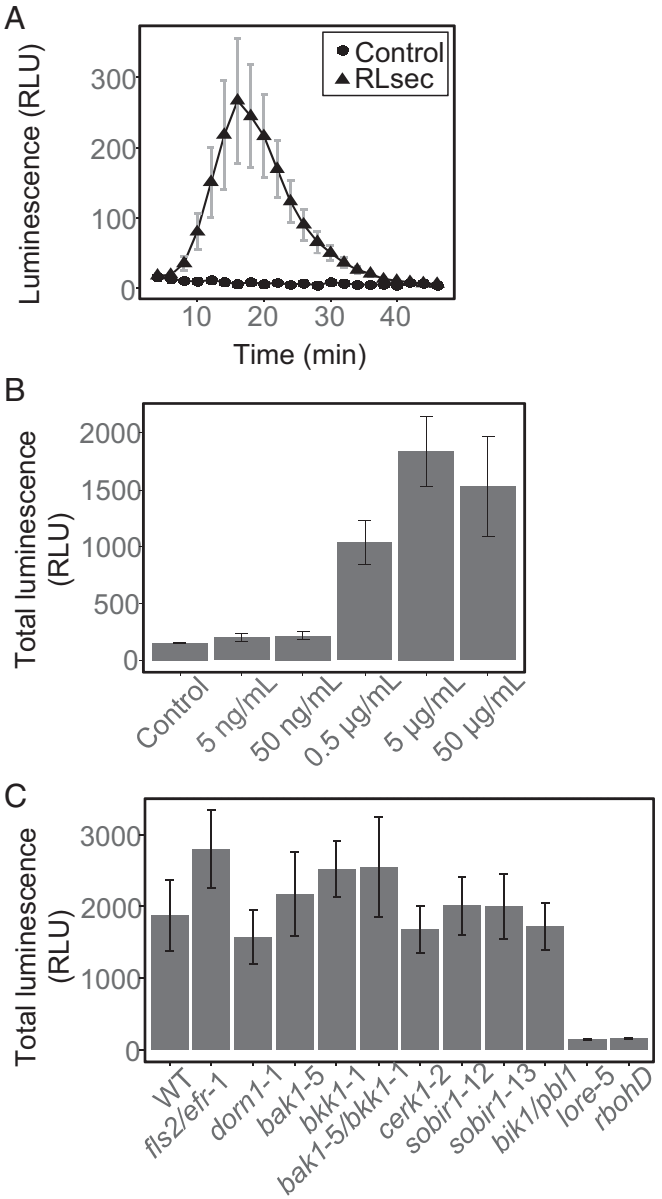

Fig. 1. RLsec activates LORE-dependent early immune-related responses in *Arabidopsis*. (*A*) Extracellular ROS production after treatment of WT leaf petioles with 50 μg/mL RLsec or EtOH as control. (*B*) Dose effect of RLsec on ROS production. ROS production measured after treatment of WT leaf petioles with the indicated concentrations of RLsec or EtOH as control. (*C*) ROS production measured after treatment of WT, *fls2*/*efr*-1, *dorn1*-1, *bak1*-5, *bkk1*-1, *bak1*-5/*bkk1*-1, *cerk1*-2, *sobir1*-12, *sobir1*-13, *bik1*/*pbl1*, *lore*-5, or *rbohD* leaf petioles with 50 μg/mL RLsec. (*A*–*C*) Data are mean ± SEM ($n = 6$). (*A*–*C*) Experiments have been realized three times with similar results.

Arabidopsis (34, 46, 47). The late ROS response triggered by mc-3-OH-FAs was dependent on LORE (34). RLsec also induced a late and long-lasting ROS burst in *Arabidopsis* culminating at 6 to 8 h posttreatment (Fig. 2*A*), which was abolished in *rbohD* but not in *lore*-5 mutant plants (Fig. 2*A*).

Next, we tested whether RLsec induces local resistance to the hemibiotrophic phytopathogen *P. syringae* pathovar (pv.) *tomato* DC3000 (*Pst)* in *Arabidopsis* (48). RLsec pretreatment significantly enhanced resistance against *Pst* infection in WT and *lore*-5 plants (Fig. 2*B*). Taken together, our results show that RLsec induces immunity-related signaling events and disease resistance in *Arabidopsis* that are partially mediated by the bulb-type lectin RK LORE.

***Pseudomonas* HAAs and mc-3-OH-FAs from RLsec Trigger LORE-Dependent *Arabidopsis* Immunity.** By contrast to RLsec, purified RLs do not trigger LORE-dependent $[Ca^{2+}]_{cyt}$ and early ROS signaling responses (34). Because RLsec contains significant amounts of HAAs, we investigated the role of these poorly studied compounds in RLsec-triggered immunity. We compared the responses to HAA with those to mc-3-OH-FAs, known to be sensed by LORE (34) and present in low amounts in RLsec (*SI Appendix*, Table S1). Side-by-side experiments with C_{10}-C_{10} HAA purified from *P. aeruginosa* secretome and 3-OH-C_{10} revealed that both compounds induce $[Ca^{2+}]_{cyt}$ signaling and ROS production in *Arabidopsis* plants in a dose-dependent manner (Fig. 3 *A* and *B* and *SI Appendix*, Figs. S4 and S5). As observed upon 3-OH-C_{10} elicitation, purified C_{10}-C_{10}–induced ROS response was impaired in *rbohD* and *lore*-5 mutants (Fig. 3*C*). Similarly, $[Ca^{2+}]_{cyt}$ signaling triggered by C_{10}-C_{10} was impaired in *lore*-5 (Fig. 3*D*). In addition, C_{10}-C_{10} and 3-OH-C_{10} both triggered LORE-dependent MPK3 and MPK6 phosphorylation (*SI Appendix*, Fig. S6*A*). WT but not *lore*-5 mutant plants pretreated with C_{10}-C_{10} or 3-OH-C_{10} displayed enhanced resistance against *Pst* (Fig. 3*E*). Similar to 3-OH-FAs (34), the acyl chain length of HAA affects its immune eliciting activity, as purified C_{14}-C_{14} from *B. glumae* neither induced ROS production nor enhanced resistance to *Pst* in *Arabidopsis* plants (*SI Appendix*, Fig. S7 *A* and *B*).

Trace amount of 3-OH-C_{10} was detected in C_{10}-C_{10} purified from *P. aeruginosa* RLsec (*SI Appendix*, Table S2). To avoid any influence of potential contamination of HAAs with eliciting compounds related to purification procedure, we tested chemically synthesized C_{10}-C_{10} for the ROS and $[Ca^{2+}]_{cyt}$ responses. Synthetic C_{10}-C_{10} triggered LORE-dependent $[Ca^{2+}]_{cyt}$ signaling and ROS production in a dose-dependent manner (Fig. 4 *A*–*C*). WT plants pretreated with synthetic C_{10}-C_{10} also displayed LORE-dependent enhanced resistance against *Pst* infection (Fig. 4*D*). LORE binds 3-OH-C_{10} through its extracellular domain (eLORE) (34). In a ligand depletion assay (*SI Appendix*, Fig. S8*A*), synthetic C_{10}-C_{10} was depleted from the low-molecular-weight fraction after size-exclusion filtration when incubated with eLORE-mCherry fusion protein transiently expressed in the apoplast of *Nicotiana benthamiana*, but not upon incubation with an apoplastic mCherry control, similarly as observed for the 3-OH-C_{10} ligand (Fig. 4*E* and *SI Appendix*, Fig. S8) (84). This strongly suggests binding of C_{10}-C_{10} to eLORE.

Altogether, our results show that HAAs secreted by *Pseudomonas* are sensed by *Arabidopsis* through the bulb-type lectin RK LORE, activate canonical PTI-related immune responses, and provide resistance to bacterial infection.

RLs Trigger LORE-Independent *Arabidopsis* Immune Responses and Resistance to *Pst*. To investigate whether RLs activate a LORE-independent immune response, we used purified Rha-Rha-C_{10}-C_{10} and Rha-C_{10}-C_{10}, the most abundant molecules from *P. aeruginosa* RLsec. In *Arabidopsis* WT, both RL congeners induced a late and long-lasting ROS production but as observed previously (34), no early burst (Fig. 5*A*). As both RL congeners gave a similar ROS signature, we only used Rha-Rha-C_{10}-C_{10} in the following experiments. The minimal concentration necessary to stimulate ROS production was 50 μM with an optimum at 100 μM (Fig. 5*B*). Late ROS production was compromised in *rbohD* but not in *lore*-5 mutants (Fig. 5*C*). Surprisingly, neither MPK3 nor MPK6 activation by Rha-Rha-C_{10}-C_{10} was detectable over a 3-h time course (*SI Appendix*, Fig. S6 *A* and *B*). L-Rhamnose alone was inactive demonstrating that the lipid part of the RLs is necessary to trigger the immune response (Fig. 5*A*). *Burkholderia* species produce RL congeners with longer lipid chains than those produced by *Pseudomonas* (15). The RLsec from phytopathogenic *Burkholderia glumae* only contains congeners with fatty acid chain lengths varying from 12 to 16 carbons, in particular Rha-Rha-C_{14}-C_{14} (49, 50). Challenge of *Arabidopsis* with purified Rha-Rha-C_{14}-C_{14} from *B. glumae* did not trigger any ROS production (Fig. 5*A*) suggesting that the length of the fatty acid chain of RLs is critical for their eliciting activity. To determine whether RLs trigger local resistance

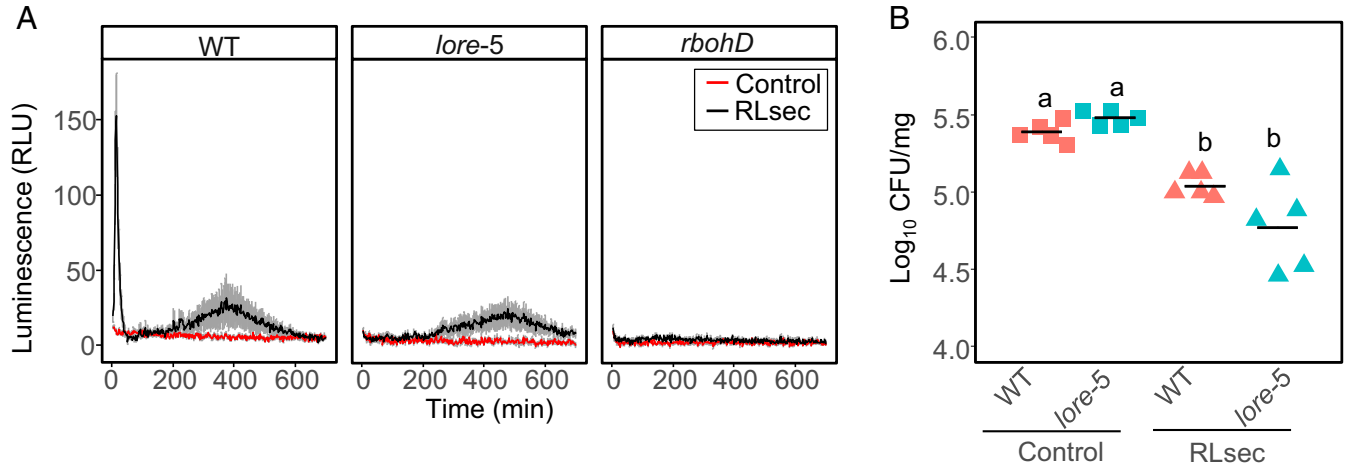

Fig. 2. RLsec activates LORE-independent responses in *Arabidopsis*. (*A*) Extracellular ROS production after treatment of WT, *lore*-5, and *rbohD* leaf petioles with 50 μg/mL RLsec or EtOH (control). ROS production was monitored over 720 min. Data are mean ± SEM ($n = 6$). Experiments have been realized three times with similar results. (*B*) WT (red) and *lore*-5 (blue) *Arabidopsis* leaves were treated with 50 μg/mL RLsec (triangle) or EtOH (square) (control) 48 h before infection. *Pst* titers were measured at 3 dpi. Data are individual data and mean (black line) ($n = 5$). Experiments have been realized three times with similar results. Letters represent results of pairwise Welch statistic test with Bonferroni correction with $P > 0.05$ (same letters) or $P \leq 0.05$ (different letters).

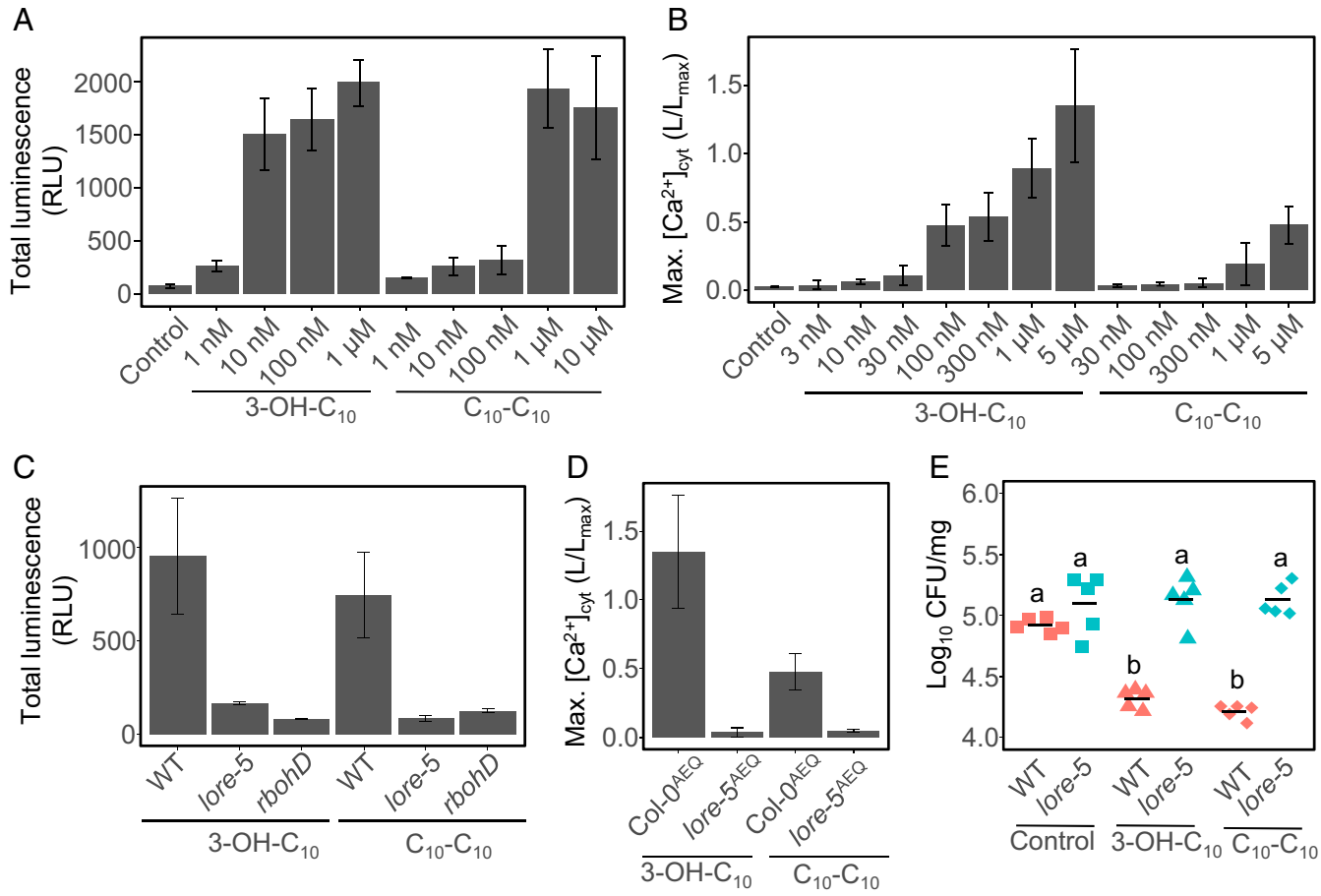

Fig. 3. Purified HAAs from *P. aeruginosa* trigger a LORE-dependent immune response in *Arabidopsis*. (*A*) Dose effect of 3-OH-C_{10} and C_{10}-C_{10} purified from *P. aeruginosa* on ROS production by WT leaf petioles. EtOH was used as negative control. Data are mean ± SEM ($n = 6$). Experiments have been realized twice with similar results. (*B*) Maximum (max.) increases in $[Ca^{2+}]_{cyt}$ in *Arabidopsis* Col-0^{AEQ} seedlings treated with different concentrations of 3-OH-C_{10}, C_{10}-C_{10} purified from *P. aeruginosa*, or MeOH as control. Data are mean ± SD ($n = 3$). Experiments have been realized twice with similar results. (*C*) ROS production measured after treatment of WT, *lore*-5, or *rbohD* leaf petioles with 10 µM 3-OH-C_{10}, 10 µM purified C_{10}-C_{10}, or EtOH as control. Data are mean ± SEM ($n = 6$). Experiments have been realized three times with similar results. (*D*) Max. increases in $[Ca^{2+}]_{cyt}$ in *Arabidopsis* Col-0^{AEQ} and *lore*-5^{AEQ} seedlings treated with 5 µM 3-OH-C_{10} or purified C_{10}-C_{10}. Data are mean ± SD ($n = 3$). Experiments have been realized twice with similar results. For *B* and *D*, the same Col-0^{AEQ} 5 µM data are presented (same experiments). (*E*) WT (red) and *lore*-5 (blue) *Arabidopsis* leaves were treated with 10 µM 3-OH-C_{10} (triangle), 10 µM purified C_{10}-C_{10} (diamond), or EtOH (square) (control) 48 h before infection. *Pst* titers were measured at 3 dpi. Data are individual data and mean (black line) ($n = 5$). Experiments have been realized twice with similar results. Letters represent results of pairwise Welch statistic test with Bonferroni correction with $P > 0.05$ (same letters) or $P \leq 0.05$ (different letters).

to pathogenic *Pseudomonas* independent of LORE, plants were pretreated with 10 µM purified Rha-Rha-C_{10}-C_{10} before *Pst* inoculation. WT plants displayed a significant enhanced resistance against *Pst* that was not compromised in *lore*-5 mutants (Fig. 5*D*).

To get deeper insights into the mechanisms involved in RL sensing, we used *Arabidopsis* plants carrying loss-of-function mutations in genes encoding RK and RLPs but also plasma membrane channel mutants including quintuple mechano-sensitive channels of small conductance-like (*msl4/5/6/9/10*) and double mid1-complementing activity (*mca1/2*) channel mutants (51) that could monitor changes in membrane mechanical properties. None of these mutants were affected in the long-term ROS response (Fig. 6*A*). Glycosylinositol phosphorylceramide (GIPC) sphingolipids were recently involved in the sensing of microbial necrosis and ethylene-inducing peptide 1-like (NLP) proteins (52). We found that the fatty acid hydroxylase *fah1/2* mutant that is disturbed in its complex sphingolipid composition (52) showed a reduced long-term ROS response (Fig. 6*B*). Ion leakage measurement confirmed that *fah1/2* mutant plants were less affected than WT plants by RL treatment (Fig. 6*C*). *fah1/2* plants are known to be more resistant to obligate biotrophic pathogens (85). We also observed that these mutants were more resistant to *Pst* (Fig. 6*D*). However, unlike in WT plants, challenge of *fah1/2* with RLs did not trigger enhanced resistance to *Pst* in the mutants, confirming that RL-triggered responses are compromised in these plants (Fig. 6*D*). Ceramide synthase *loh1* mutants are also impaired in GIPC levels but not in glucosyl ceramides (52). Interestingly, RL-triggered ROS production and ion leakage was unaltered in *loh1* plants. Altogether, our results show that RLs activate an atypical immune response in *Arabidopsis* that is LORE independent but which is affected by the sphingolipid composition of the plasma membrane.

Discussion

In *Pseudomonas* and *Burkholderia* species, swarming motility is intimately related to the production of extracellular surface-active RLs and HAAs (22, 25, 53–55). In addition, RL production affects bacterial biofilm architecture and increases affinity of cells for initial adherence to surfaces through increasing the cell's surface hydrophobicity (19, 56). These exoproducts are therefore at the frontline during host colonization. Our work demonstrates that both RLs and HAAs from the *Pseudomonas* lipidic

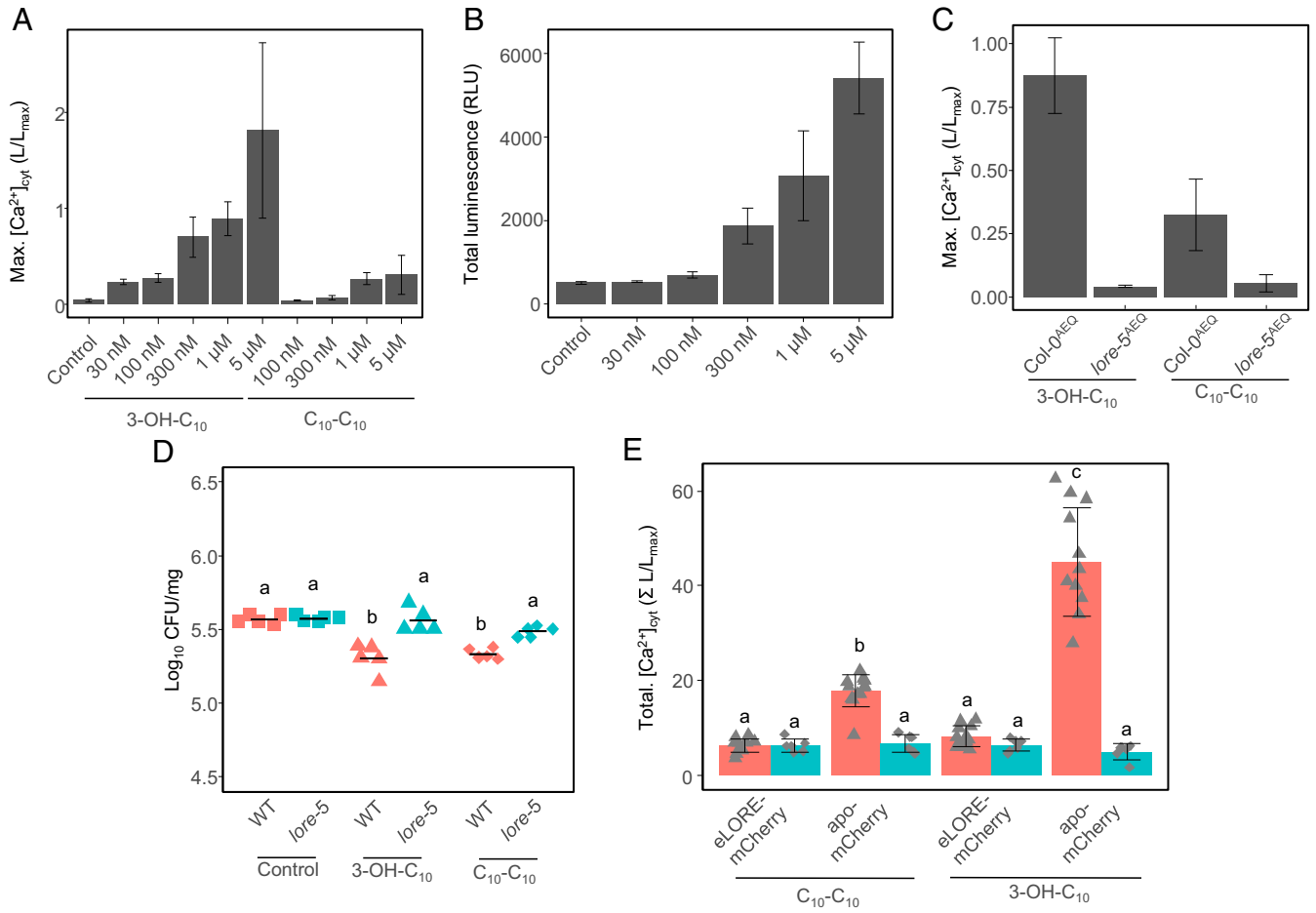

Fig. 4. Synthetic HAAs trigger a LORE-dependent immune response in *Arabidopsis*. (*A*) Maximum (max.) increases in $[Ca^{2+}]_{cyt}$ in *Arabidopsis* Col-0^{AEQ} seedlings treated with different concentrations of 3-OH-C_{10}, synthetic C_{10}-C_{10}, or MeOH. Data are mean ± SD ($n = 3$). Experiments have been realized twice with similar results. (*B*) Dose effect of synthetic C_{10}-C_{10} on ROS production by WT leaf petioles. EtOH was used as negative control. Data are mean ± SEM ($n = 6$). Experiments have been realized twice with similar results. (*C*) Max. increases in $[Ca^{2+}]_{cyt}$ in *Arabidopsis* Col-0^{AEQ} and *lore*-5^{AEQ} seedlings treated with 5 µM 3-OH-C_{10} or synthetic C_{10}-C_{10}. Data are mean ± SD ($n = 3$). Experiments have been realized twice with similar results. (*D*) WT (red) and *lore*-5 (blue) *Arabidopsis* leaves were treated with 10 µM 3-OH-C_{10} (triangle), 10 µM synthetic C_{10}-C_{10} (diamond), or MeOH (square) (control) 48 h before infection. *Pst* titers were measured at 3 dpi. Data are individual data and mean (black line) ($n = 5$). Experiments have been realized twice with similar results. Letters represent data of pairwise Welch statistic test with Bonferroni correction with $P > 0.05$ (same letters) or $P \leq 0.05$ (different letters). (*E*) Depletion of 1 µM synthetic C_{10}-C_{10} or 100 nM 3-OH-C_{10} by concentrated apoplastic wash fluid from *N. benthamiana* containing LORE extracellular domain (eLORE)-mCherry fusion protein or apoplastic (apo)-mCherry as control as illustrated in *SI Appendix*, Fig. S8*A*. Unbound ligand content in low-molecular-weight filtrate was analyzed by $[Ca^{2+}]_{cyt}$ measurements in LORE-overexpressing (red bars, gray triangles, $n = 12$) and *lore*-1 (blue bars, gray diamonds, $n = 6$) *Arabidopsis* seedlings. Data are mean ± SD and individual data of three pooled experiments. Letters represent data of pairwise Wilcoxon statistic test with Bonferroni correction with $P > 0.05$ (same letters) or $P \leq 0.05$ (different letters).

secretome, referred to as RLsec here, are able to trigger *Arabidopsis* innate immunity by two distinct mechanisms.

We found that *Pseudomonas* RLs induce an atypical immune response. This response does not involve the RK LORE. Other bacterial compounds comprising mc-3-OH-acyl building blocks, but with large decorations including lipid A or LPS, lipopeptides, and *N*-acyl homoserine lactones, also do not trigger LORE-dependent immune responses (34). RLs are glycolipids made of L-rhamnose linked to an HAA lipid tail (15, 21). Therefore, we propose that glycosylation of HAAs abolishes their perception by LORE. Glycosylation is known to affect the perception of IPs. Glycosylation of the flagellin from *Acidovorax avenae* on Ser^{178} and Ser^{183} prevents its perception by rice cells (57). Similarly, unglycosylated flagellin from *P. syringae* pv. *tabaci* 6605 induces stronger defense responses in tobacco plants than glycosylated flagellin (58). In humans, glycosylation of *Burkholderia cenocepacia* flagellin significantly reduces its perception by epithelial cells (59).

We found that RL perception does not involve previously characterized RKs, RLPs, or mechanosensitive channels. However, the RL response is affected by alterations in sphingolipid synthesis suggesting a role of these key membrane lipids in RL-triggered immunity. Recently GIPCs, major structural components of the plant plasma membrane together with glucosylceramides (GlcCers), have been involved as receptors of cytotoxic NLPs (52). NLPs bind terminal monomeric hexose moieties of GIPCs. Only eudicot plants are sensing these NLPs through sphingolipid receptors. Insensitivity of monocots to NLPs is due to the length of the GIPC headgroup, consisting of three terminal hexoses compared to two in eudicots (52). *fah1/2* mutants display reduced glycosylsphingolipid (GIPCs and GlcCers) content but also a lower level of ordered plasma membranes (52), suggesting that, similar to the NLP response, complex sphingolipids and/or ordered plasma membranes are necessary for the RL response. Unlike NLPs, RL responses were not significantly affected in *loh1* mutant plants also suggesting that GlcCers more

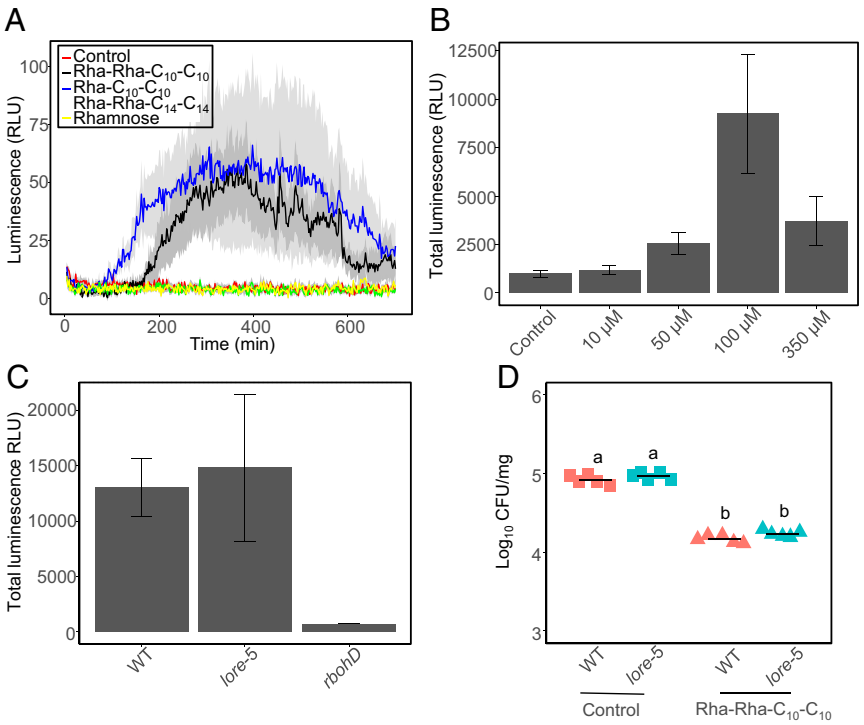

Fig. 5. Purified RLs trigger a LORE-independent *Arabidopsis* immune response. (*A*) Extracellular late ROS production after treatment of WT leaf petioles with 100 µM RLs, 100 µM L-rhamnose, or EtOH (control). Data are mean ± SEM ($n = 6$). (*B*) Dose effect of Rha-Rha-C_{10}-C_{10} on late ROS production. ROS production measured after treatment of WT leaf petioles with the indicated concentrations of Rha-Rha-C_{10}-C_{10} or EtOH (control). Data are mean ± SEM ($n = 6$). (*C*) Late ROS production measured after treatment of WT, *lore*-5, or *rbohD* leaf petioles with 100 µM Rha-Rha-C_{10}-C_{10}. Data are mean ± SEM ($n = 6$). (*D*) WT (red) and *lore-5* (blue) *Arabidopsis* leaves were treated with 10 µM Rha-Rha-C_{10}-C_{10} (triangle) or EtOH (square) (control) 48 h before infection. *Pst* titers were measured at 3 dpi. Data are individual data and mean (black line) ($n = 5$). Letters represent results of pairwise *t* statistic test with Bonferroni correction with $P > 0.05$ (same letters) or $P \leq 0.05$ (different letters). (*A–D*) Experiments have been realized three times with similar results.

than GIPC could influence RL sensing (52). Surfactin and more recently synthetic RL bolaforms and synthetic glycolipids, also active in the micromolar range, have been proposed to directly interact with plasma membrane lipids (46, 60–62). Mono- and di-RLs from *Pseudomonas* interact with phospholipids in several synthetic membrane systems (63–66). In particular, RLs are able to fit into phospholipid bilayers of plant biomimetic plasma membranes (67). In this model, the rhamnose polar heads from RLs are located near the phosphate groups from phospholipids, and RL hydrophobic lipid tails are surrounded by the lipid chains from these phospholipids (67). The results obtained with these plant plasma membrane models suggest that the insertion of RLs into the lipid bilayer does not significantly affect lipid dynamics. The nature of the phytosterols could however influence the RL effect on plant plasma membrane destabilization. Subtle changes in lipid dynamics could then be linked to plant defense induction (67). Interestingly, RL bolaforms, like natural RLs, are inducing a noncanonical defense signature with a long-lasting oxidative burst without MPK3 or MPK6 activation (46). We showed that the late ROS response triggered by RLs and RL-bolaforms is fully dependent on RBOHD, which differs from the second ROS response observed after LPS treatment and produced by chloroplasts (47). The RL-related ROS response is not directly linked to *Arabidopsis* protection to *Pst* as some bolaforms can trigger this late ROS production without increasing resistance to *Pst* (46). However, the experiments from Luzuriaga-Loaiza et al. (46) and our results on natural RLs suggest that the late ROS response is closely linked to ion leakage and may therefore be involved in membrane destabilization. This atypical defense signature triggered by two structurally different RLs, displaying amphiphilic properties and biological activities at the micromolar range, may suggest a direct interaction of these molecules with plant plasma membrane lipids, similar to what has been shown on membrane models (46).

We also demonstrated that HAAs, found in large amount in *Pseudomonas* lipidic secretome, are IPs perceived by *Arabidopsis*. HAA sensing is mediated by LORE. HAAs, in the micromolar range, induce typical PTI responses including transient ROS production, $[Ca^{2+}]_{cyt}$ signaling, and MPK3 and MPK6 phosphorylation in *Arabidopsis.* Interestingly, 3-OH-C_{10} activates similar responses but at concentrations 10 to 50 times lower. This is intriguing because HAAs are present in much larger quantities (more than 3%) compared to 3-OH-FAs (0.3%) in the lipidic secretome (*SI Appendix*, Table S1). This high amount of HAAs may compensate for their lower activity. RLs are activating an immune response at relatively high concentrations compared to both compounds. Interestingly, the RL concentration in the *P. aeruginosa* lipidic secretome is 10 to 100 times higher than HAAs and usually is in the millimolar range (23, 68). RLs are produced between 20 and 110 µM in vivo in mammals infected by *P. aeruginosa*, especially during cystic fibrosis disease (69–71). The high concentrations of RLs needed for plant elicitation are in the range of the concentrations produced by the bacteria.

Higher steric hindrance of HAA compared to 3-OH-FAs likely results in a lower affinity to the LORE receptor. Synthetic ethyl 3-hydroxydecanoate (Et-3-OH-C10:0) and *n*-butyl 3-hydroxydecanoate (*n*But-3-OH-C10:0), which possess unbranched ester-bound carbon chains in place of the carboxyl group, also triggered LORE-dependent immune signaling in *Arabidopsis*, while 3-branched *tert*-butyl 3-hydroxydecanoate (*t*But-3-OH-C10:0) was inactive (34). HAAs, possessing a 2-branched ester-bound headgroup, activate LORE signaling. The differences in efficacy could be explained by the

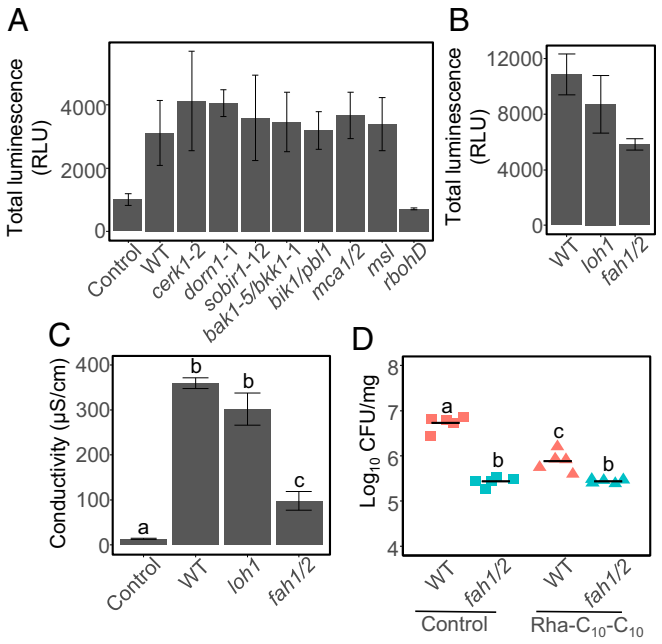

Fig. 6. RL perception is impacted by plasma membrane sphingolipid composition. Extracellular late ROS production after treatment of (*A*) WT, *cerk1*-2, *dorn1*-1, *sobir1*-12, *bak1*-5/*bkk1*-1, *bik1*/*pbl1*, *mca1*/*2*, *msl4*/*5*/*6*/*9*/*10* (*msl*), or *rbohD,* and (*B*) WT, *loh1*, or *fah1*/*2 Arabidopsis* leaf petioles with 100 µM Rha-Rha-C_{10}-C_{10} or EtOH (control). Data are mean ± SEM (n = 6). Experiments have been realized three times with similar results. (*C*) Electrolyte leakage induced by 100 µM Rha-C_{10}-C_{10} or EtOH (control) on WT, *loh1*, or *fah1*/*2 Arabidopsis* leaf discs 24 h posttreatment. Data are mean ± SEM (n = 6). Letters represent results of pairwise Wilcoxon Mann–Whitney U statistic test with $P > 0.05$ (same letters) or $P \leq 0.05$ (different letters). Experiments have been realized twice with similar results. (*D*) WT (red) and *fah1*/*2* (blue) *Arabidopsis* leaves were treated with 10 µM Rha-C_{10}-C_{10} (triangle) or EtOH (square) (control) 48 h before infection. *Pst* titers were measured at 3 dpi. Data are individual data and mean (black line) (n = 5). Letters represent results of pairwise Welch statistic test with Bonferroni correction with $P > 0.05$ (same letters) or $P \leq 0.05$ (different letters).

different steric hindrance of the molecules. Alternatively, the additional carboxyl group could account for the LORE-eliciting activity of HAAs.

Pantoea, *Dickeya*, and *Pseudomonas* bacteria, in particular the well-known phytopathogen *P. syringae*, mainly produce HAAs containing 3-hydroxydecanoic acid (C_{10}) tails (15, 22, 72). By contrast, *Burkholderia* species including the phytopathogenic bacterium *B. glumae* mainly produce HAAs comprising 3-hydroxytetradecanoic acid (C_{14}) tails (49). *Pseudomonas* C_{10}-containing HAAs activated *Arabidopsis* PTI whereas *Burkholderia* HAAs containing C_{14} fatty acid did not. Chain-length specificity was also observed for mc-3-OH-FA sensing by the LORE receptor with 3-OH-C_{10} representing the strongest immune elicitor (34). Thus, it could be hypothesized that *Arabidopsis*, and more generally *Brassicaceae* (73), are able to specifically recognize HAAs from specific bacterial species, among which several are plant opportunistic and phytopathogens (74–77). Interestingly, transcript profiles of the bean pathogen *P. syringae* pv. *syringae* B728a support a model in which leaf surface or epiphytic sites specifically favor swarming motility based on HAA surfactant production (55, 78). Low levels of HAAs contributing to motility are produced by these bacteria (22). HAA concentrations necessary to stimulate *Arabidopsis* innate immunity are in line with the concentration detected in RLsec and are produced by *Pseudomonas* (between 3 to 20% of the secretome) (23, 68, 79).

Low amounts of free mc-3-OH-FAs were found in RLsec from *P. aeruginosa* (*SI Appendix*, Table S1). In *Pseudomonas*, the outer membrane lipase PagL releases 3-OH-C_{10} during synthesis of penta-acylated lipid A (34). The further fate of this 3-OH-C_{10} is unknown. RLs are able to extract LPS from the outer membrane of *P. aeruginosa* (27). Conceivably, surface-active RLs, and presumably also HAAs, could release free 3-OH-C_{10}, produced through PagL activity, along with LPS from the bacterial cell wall or outer membrane vesicles (27). Alternatively, degradation of HAAs/RLs in planta may also release free 3-OH-C_{10}. Acyl carrier protein (ACP)- and coenzyme A (CoA)-bound mc-3-OH-FAs are precursors of HAA/RL synthesis (21). Upon bacterial cell lysis, enzymatic or nonenzymatic degradation processes may also generate free 3-OH-C_{10} from these precursors. In vivo, insights into IP release have been recently obtained for flagellin. The plant glycosidase BGAL1 facilitates the release of immunogenic peptides from glycosylated flagellin, upstream of cleavage by proteases (80). The pathogen may evade detection by altering flagellin glycosylation and inhibiting the plant glycosidase. Flagellin glycosylation increases its physical stability that could contribute to the nonliberation/recognition of the flg22 epitope (58, 81). RLs are able to shed flagellin from *P. aeruginosa* flagella (26), suggesting that these biosurfactants participate in the release of this and presumably other eliciting compounds.

In conclusion, we hypothesize that when HAA- and RL-producing *Pseudomonas* colonize the leaf or root surface, they release RLs and HAAs, which are necessary for surface motility, biofilm development, and thus successful colonization. Whereas *Arabidopsis* senses HAAs and mc-3-OH-FAs through the bulb-type lectin receptor kinase LORE, RLs are perceived through a LORE-independent mechanism (Fig. 7). In addition to direct activation of a noncanonical defense response in plants, RLs, by releasing other IPs from bacteria, could orchestrate a node leading to strong activation of plant immunity.

Methods

Molecules. The *P. aeruginosa* lipidic secretome used in this study was obtained from Jeneil Biosurfactant Co. (JBR-599, lot no. 050629). Rha-Rha-C_{10}-C_{10} and Rha-C_{10}-C_{10} were purified from this lipidic secretome mixture, as previously described (33, 34). Rha-Rha-C_{14}-C_{14} were purified from the *B. glumae* lipidic secretome (49). To obtain pure HAAs from *P. aeruginosa* or *B. glumae*, RLs were hydrolyzed using 1 M HCl in 1:1 dioxane–water boiling at reflux for 60 min. The mixture was extracted with ethyl acetate, and the extracts were dried over anhydrous Na_2SO_4. After filtration, the resulting extracts were then evaporated to dryness and resuspended in 2 mL methanol. HAAs were then isolated from digested mixture using flash chromatography on a Biotage Isorela One instrument with a SNAP Ultra C18 12 g column (Biotage) using an acetonitrile/water gradient at 12 mL/min flow rate. The elution was started with 0% acetonitrile for 4.5 min, and the acetonitrile concentration was raised to 100% over 28.2 min, followed by an isocratic elution of 100% acetonitrile for 13.3 min. The flash chromatography fraction containing the C_{10}-C_{10} was further separated and purified using 0.25-mm thin-layer chromatographic plates (SiliCycle SilicaPlate F-254) and developed with *n*-hexanes-ethyl acetate-acetic acid (24:74:2). The bands were scraped from the plates, and the HAAs, including C_{10}-C_{10}, were extracted from the silica with chloroform-methanol (5:1). 3-OH-C_{10} was purchased from Sigma-Aldrich. All compounds were dissolved in ethanol or methanol as indicated to prepare stock solutions. Final aqueous compound dilutions were prepared freshly on the days of the experiment. Control solutions contained equal amounts of ethanol or methanol (0.05% for most experiments and not exceeding 0.5% for the highest concentrations tested). Chemical synthesis and HPLC purification of C_{10}-C_{10} is described in Datasets S1 and S2.

LC-MS Analysis of HAAs. Samples were prepared by diluting stock solutions using MeOH to final concentration of 50 parts per million (ppm). 16-Hydroxyhexadecanoic acid at 20 ppm was added to samples as internal standard (68). The analyses were performed with a Quattro II triple quadrupole mass spectrometer (Micromass) equipped with a Z-spray interface using electrospray ionization in negative mode. The capillary voltage was set at 3.5 kV and the cone voltage at 25 V. The source temperature was kept at 120 °C and the desolvation gas at 150 °C. The scanning mass range was from

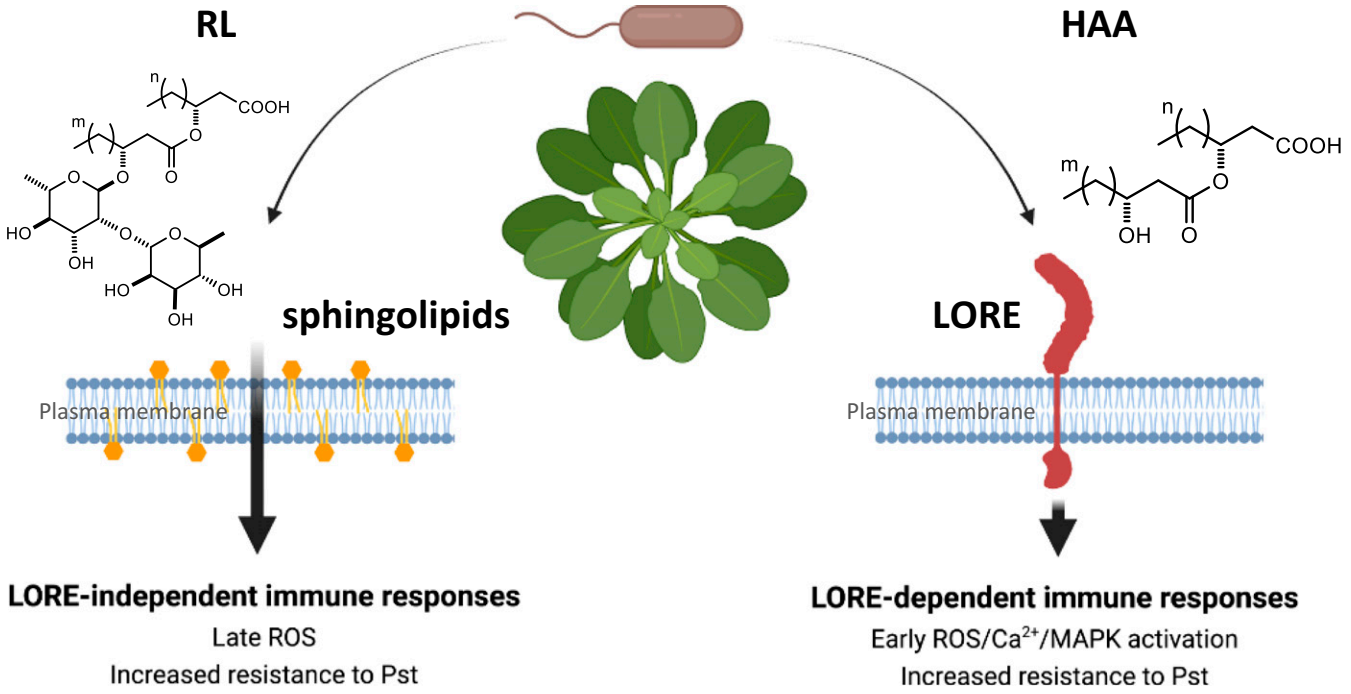

Fig. 7. Proposed model for HAA and rhamnolipid perception mechanisms in *Arabidopsis* and integrated immune responses. RL-producing bacteria excrete rhamnolipids and HAAs to form biofilm and for successful colonization. *Arabidopsis* perceives HAAs via LORE and rhamnolipids by a LORE-independent pathway affected by sphingolipids composition of the plant plasma membrane, resulting in the activation of efficient immune responses. Parts of this scheme were created with https://BioRender.com.

130 to 930 Da. The instrument was interfaced to an HPLC (Waters 2795) equipped with a 100 × 4 mm internal diameter (i.d.) Luna Omega PS C18 reversed-phase column (particle size 5 μm) using a water-acetonitrile gradient with a constant 2 mmol/L^{-1} concentration of ammonium acetate (0.6 mL/min^{-1}). Quantification of free 3-OH-C_{10} in purified C_{10}-C_{10}, Rha-Rha-C_{10}-C_{10}, Rha-C_{10}-C_{10}, Rha-Rha-C_{14}-C_{14}, or synthetic C_{10}-C_{10} was performed as reported previously (34) and are presented in *SI Appendix*, Table S2.

Plant Material and Growth Conditions. *Arabidopsis thaliana* ecotype Col-0 was used as WT parent for all experiments. Seeds from *fls2/efr*-1 (38, 39), *bak1*-5, *bkk1*-1, *bak1-5/bkk1-1* (40), *cerk1-2* (42), *bik1/pbl1* (41), *rbohD, msl4/5/6/9/10*, and *mca1/2* (51) were provided by C. Zipfel. Seeds from *sobir1*-12 and *sobir1*-13 (43) were provided by F. Brunner (Center for Plant Molecular Biology, University of Tübingen, Tübingen, PlantResponse). Seeds from *sd1-29* (*lore-5*), Col-0^{AEQ}, and *lore*-5^{AEQ} were provided by S. Ranf (45). *loh1* and *fah1/2* seed (52) were provided by I. Feussner (University of Göttingen, Germany). *dorn1*-1 seeds (44) were obtained from NASC stock (SALK_042209). All mutants are in the Col-0 background. Plants were grown on soil in growth chambers at 20 °C, under 12-h light/12-h dark regime with fluorescent light of 150 μmol/m^{-2}/s^{-1} and 60% relative humidity.

Extracellular ROS Production and Calcium Signaling. ROS assays were performed on 4- to 6-wk-old *Arabidopsis* plants cultured on soil. Briefly, 5-mm-long petiole sections were cut and placed in 150 μL distilled water overnight in 96-wells plate (PerkinElmer) (46). Then, the protocol was conducted as previously described (82). Luminescence (relative light units, RLU) was measured every 2 min during 46 or 720 min with a Tecan Infinite F200 PRO (or a TECAN CM SPARK for *SI Appendix*, Fig. S6), Tecan. Total ROS production was calculated by summing RLU measured between 4 to 46 or 4 to 720 min after treatment. Control was realized on petioles of WT or mutant plants. $[Ca^{2+}]_{cyt}$ measurements were done as previously described (34).

MAPK Phosphorylation Assays. For MAPK phosphorylation assays, three leaf disks (9-mm diameter) were collected from 4- to 6-wk-old *Arabidopsis* plants grown on soil and incubated 8 h in distilled water. Leaf disks were mock treated or treated with different molecules. Fifteen minutes, 1 h, and 3 h after treatment, plant tissues were frozen in liquid nitrogen. To extract proteins, 60 mg leaf tissues were ground in a homogenizer Potter-Elvehjem with 60 μL extraction buffer (0.35 M Tris HCl [pH 6.8], 30% [volume(vol)/vol] glycerol, 10% [vol/vol] sodium dodecyl sulfate [SDS], 0.6 M dithiothreitol [DTT], 0.012% [weight/vol] bromophenol blue). Total protein extracts were denatured for 7 min at 95 °C, centrifuged at 11,000 *g* for 5 min, and 30 μL supernatant was separated by 12% SDS-polyacrylamide gel electrophoresis (PAGE). Phosphorylation state of MAPKs by immunobloting was performed as previously described (46).

Depletion Binding Assay. Protein expression and ligand depletion were performed as described (84) with slight modifications. Briefly, LORE extracellular domain mCherry fusion protein (eLORE-mCherry) or mCherry control fused with N-terminal LORE signal peptide were transiently expressed in *N. benthamiana* leaf apoplast using a 1:1 mixture of *Agrobacterium tumefaciens* GV3101 carrying the respective expression plasmid or the p19 silencing suppressor (total optical density $[OD]_{600}$ 0.5). At 5 d postinoculation, *N. benthamiana* leaves were vacuum infiltrated with water, and apoplastic washing fluid (AWF) was collected by centrifugation (20 min, 800 *g*, 4 °C). AWF was cleared by centrifugation (20 min, 8,000 *g*, 4 °C), filter sterilized (pore size 0.22 μm), desalted (PD-10 Desalting Columns, Cytiva), and concentrated to a total protein concentration of 2 mg/mL (Vivaspin 20, 30,000 Da molecular weight [MW] cutoff, Sartorius). For ligand depletion assay, AWF concentrate was mixed in 9:1 ratio (vol:vol) with synthetic C_{10}-C_{10} (50 μM) or 3-OH-C_{10} (5 μM) and incubated for 1 h at 4 °C on a rotator. Unbound ligands were separated from the mixture (Vivaspin 500, 30,000 Da MW cutoff, Sartorius). Content of unbound C_{10}-C_{10} and 3-OH-C_{10} in filtrates was assessed by $[Ca^{2+}]_{cyt}$ measurements using LORE-overexpressing (*p35S:LORE/lore*-1) and *lore*-1 seedlings with a filtrate:water ratio of 1:4 (vol:vol).

Conductivity Assay. The assay was performed as described previously (83), with few modifications. Eight leaf discs of 6-mm diameter were incubated in distilled water overnight. One disk was transferred into a 1.5-mL tube containing fresh distilled water and the corresponding elicitor concentration or ethanol for control. Conductivity measurements (three to four replicates for each treatment) were then conducted using a B-771 LaquaTwin (Horiba) conductivity meter.

***P. syringae* Culture and Disease-Resistance Assays.** *P. syringae* pv. *tomato* strain DC3000 was grown at 28 °C under stirring in King's B (KB) liquid medium supplemented with antibiotics: 50 μg/mL^{-1} rifampicin and 50 μg/mL^{-1} kanamycin. For local protection assays, 15 seeds were sown per pot and grown for 3 to 5 wk in soil. Plants were sprayed with molecules or ethanol as control and

were placed for 2 d in high humidity atmosphere before infections. Plants were inoculated by spraying the leaves with 3 mL bacterial suspension at an OD_{600} of 0.01 (0.025% Silwet L-77, 10 mM $MgCl_2$). For each experiment, five pots per conditions were used ($n = 5$). Quantification (colony forming units [CFU]) of in planta bacterial growth was performed 3 days post infection (dpi). To this end, all plant leaves from the same pot were harvested, weighed, and crushed in a mortar with 10 mL of 10 mM $MgCl_2$, and serial dilutions were performed. For each dilution, 10 µL were dropped on KB plate supplemented with appropriate antibiotics. CFU were counted after 2 d of incubation at 28 °C. The number of bacteria per milligram of plants fresh mass was obtained with the following formula:

$$\mathrm{CFU.mg^{-1}} = \frac{\left(\frac{N \times Vd}{Vi} \times 10^{(n-1)} \times 100\right)}{M},$$

with N equal to CFU number, Vi the volume depot on plate, Vd the total volume, n the dilution number, and M the plants fresh mass.

Data Availability. All study data are included in the article and/or supporting information.

ACKNOWLEDGMENTS. We are thankful to Laetitia Parent and Sylvain Milot for technical support and Ralph Hückelhoven for critical discussion. This work was supported by grants from EliDeRham and Rhamnoprot (Région Grand Est). The project Rhamnoprot is cofunded by the European Union FEDER (Fonds Européens de Développement Régional) program. Financial support from the CNRS, the MESRI (Ministère de l'Enseignement Supérieur, de la Recherche et de l'Innovation), and the Federative Research Structure SFR Condorcet are gratefully acknowledged. Works on rhamnolipids in the E.D. and C.G. laboratories are funded by the Natural Sciences and Engineering Research Council of Canada (NSERC) through Discovery Grants RGPIN-2015-03931 and RGPIN-2020-06771 (to E.D.) and RGPIN-2016-04950 (to C.G.). Work in the S.R. laboratory is supported by the German Research Foundation (SFB924/TP-B10 and Emmy Noether programme RA2541/1). M.C. thanks The Natural Sciences and Engineering Research Council of Canada (NSERC) and Fonds de Recherche du Québec – Nature et Technologies (FRQNT) for M.Sc. and Ph.D. scholarships.

1. D. E. Cook, C. H. Mesarich, B. P. Thomma, Understanding plant immunity as a surveillance system to detect invasion. *Annu. Rev. Phytopathol.* **53**, 541–563 (2015).
2. K. Kanyuka, J. J. Rudd, Cell surface immune receptors: The guardians of the plant's extracellular spaces. *Curr. Opin. Plant Biol.* **50**, 1–8 (2019).
3. T. Boller, G. Felix, A renaissance of elicitors: Perception of microbe-associated molecular patterns and danger signals by pattern-recognition receptors. *Annu. Rev. Plant Biol.* **60**, 379–406 (2009).
4. M. A. Newman, T. Sundelin, J. T. Nielsen, G. Erbs, MAMP (microbe-associated molecular pattern) triggered immunity in plants. *Front. Plant Sci.* **4**, 139 (2013).
5. F. Boutrot, C. Zipfel, Function, discovery, and exploitation of plant pattern recognition receptors for broad-spectrum disease resistance. *Annu. Rev. Phytopathol.* **55**, 257–286 (2017).
6. S. Ranf, Sensing of molecular patterns through cell surface immune receptors. *Curr. Opin. Plant Biol.* **38**, 68–77 (2017).
7. D. Couto, C. Zipfel, Regulation of pattern recognition receptor signalling in plants. *Nat. Rev. Immunol.* **16**, 537–552 (2016).
8. J. Bigeard, J. Colcombet, H. Hirt, Signaling mechanisms in pattern-triggered immunity (PTI). *Mol. Plant* **8**, 521–539 (2015).
9. A. Garcia-Brugger *et al*., Early signaling events induced by elicitors of plant defenses. *Mol. Plant Microbe Interact.* **19**, 711–724 (2006).
10. S. Wu, L. Shan, P. He, Microbial signature-triggered plant defense responses and early signaling mechanisms. *Plant Sci.* **228**, 118–126 (2014).
11. D. De Vleesschauwer, G. Gheysen, M. Höfte, Hormone defense networking in rice: Tales from a different world. *Trends Plant Sci.* **18**, 555–565 (2013).
12. J. Glazebrook, Contrasting mechanisms of defense against biotrophic and necrotrophic pathogens. *Annu. Rev. Phytopathol.* **43**, 205–227 (2005).
13. A. Robert-Seilaniantz, M. Grant, J. D. Jones, Hormone crosstalk in plant disease and defense: More than just jasmonate-salicylate antagonism. *Annu. Rev. Phytopathol.* **49**, 317–343 (2011).
14. L. Trdá *et al*., Perception of pathogenic or beneficial bacteria and their evasion of host immunity: Pattern recognition receptors in the frontline. *Front. Plant Sci.* **6**, 219 (2015).
15. A. M. Abdel-Mawgoud, F. Lépine, E. Déziel, Rhamnolipids: Diversity of structures, microbial origins and roles. *Appl. Microbiol. Biotechnol.* **86**, 1323–1336 (2010).
16. V. U. Irorere, L. Tripathi, R. Marchant, S. McClean, I. M. Banat, Microbial rhamnolipid production: A critical re-evaluation of published data and suggested future publication criteria. *Appl. Microbiol. Biotechnol.* **101**, 3941–3951 (2017).
17. M. Perneel *et al*., Phenazines and biosurfactants interact in the biological control of soil-borne diseases caused by *Pythium* spp. *Environ. Microbiol.* **10**, 778–788 (2008).
18. Ł. Chrzanowski, Ł. Ławniczak, K. Czaczyk, Why do microorganisms produce rhamnolipids? *World J. Microbiol. Biotechnol.* **28**, 401–419 (2012).
19. A. Nickzad, E. Déziel, The involvement of rhamnolipids in microbial cell adhesion and biofilm development–An approach for control? *Lett. Appl. Microbiol.* **58**, 447–453 (2014).
20. P. Vatsa, L. Sanchez, C. Clément, F. Baillieul, S. Dorey, Rhamnolipid biosurfactants as new players in animal and plant defense against microbes. *Int. J. Mol. Sci.* **11**, 5095–5108 (2010).
21. A. M. Abdel-Mawgoud, F. Lépine, E. Déziel, A stereospecific pathway diverts β-oxidation intermediates to the biosynthesis of rhamnolipid biosurfactants. *Chem. Biol.* **21**, 156–164 (2014).
22. A. Y. Burch *et al*., *Pseudomonas syringae* coordinates production of a motility-enabling surfactant with flagellar assembly. *J. Bacteriol.* **194**, 1287–1298 (2012).
23. E. Déziel, F. Lépine, S. Milot, R. Villemur, *rhlA* is required for the production of a novel biosurfactant promoting swarming motility in *Pseudomonas aeruginosa*: 3-(3-hydroxyalkanoyloxy)alkanoic acids (HAAs), the precursors of rhamnolipids. *Microbiology (Reading)* **149**, 2005–2013 (2003).
24. J. M. Plotnikova, L. G. Rahme, F. M. Ausubel, Pathogenesis of the human opportunistic pathogen *Pseudomonas aeruginosa* PA14 in *Arabidopsis*. *Plant Physiol.* **124**, 1766–1774 (2000).
25. J. Tremblay, A. P. Richardson, F. Lépine, E. Déziel, Self-produced extracellular stimuli modulate the *Pseudomonas aeruginosa* swarming motility behaviour. *Environ. Microbiol.* **9**, 2622–2630 (2007).
26. U. Gerstel, M. Czapp, J. Bartels, J. M. Schröder, Rhamnolipid-induced shedding of flagellin from *Pseudomonas aeruginosa* provokes hBD-2 and IL-8 response in human keratinocytes. *Cell. Microbiol.* **11**, 842–853 (2009).
27. R. A. Al-Tahhan, T. R. Sandrin, A. A. Bodour, R. M. Maier, Rhamnolipid-induced removal of lipopolysaccharide from *Pseudomonas aeruginosa*: Effect on cell surface properties and interaction with hydrophobic substrates. *Appl. Environ. Microbiol.* **66**, 3262–3268 (2000).
28. J. Andrä *et al*., Endotoxin-like properties of a rhamnolipid exotoxin from *Burkholderia* (*Pseudomonas*) *plantarii*: Immune cell stimulation and biophysical characterization. *Biol. Chem.* **387**, 301–310 (2006).
29. J. Bauer, K. Brandenburg, U. Zähringer, J. Rademann, Chemical synthesis of a glycolipid library by a solid-phase strategy allows elucidation of the structural specificity of immunostimulation by rhamnolipids. *Chemistry* **12**, 7116–7124 (2006).
30. J. Dössel, U. Meyer-Hoffert, J. M. Schröder, U. Gerstel, *Pseudomonas aeruginosa*-derived rhamnolipids subvert the host innate immune response through manipulation of the human beta-defensin-2 expression. *Cell. Microbiol.* **14**, 1364–1375 (2012).
31. M. Gonzalez-Juarrero *et al*., Polar lipids of *Burkholderia pseudomallei* induce different host immune responses. *PLoS One* **8**, e80368 (2013).
32. L. Sanchez *et al*., Rhamnolipids elicit defense responses and induce disease resistance against biotrophic, hemibiotrophic, and necrotrophic pathogens that require different signaling pathways in *Arabidopsis* and highlight a central role for salicylic acid. *Plant Physiol.* **160**, 1630–1641 (2012).
33. A. L. Varnier *et al*., Bacterial rhamnolipids are novel MAMPs conferring resistance to *Botrytis cinerea* in grapevine. *Plant Cell Environ.* **32**, 178–193 (2009).
34. A. Kutschera *et al*., Bacterial medium-chain 3-hydroxy fatty acid metabolites trigger immunity in *Arabidopsis* plants. *Science* **364**, 178–181 (2019).
35. J. Qi, J. Wang, Z. Gong, J. M. Zhou, Apoplastic ROS signaling in plant immunity. *Curr. Opin. Plant Biol.* **38**, 92–100 (2017).
36. Y. Kadota, K. Shirasu, C. Zipfel, Regulation of the NADPH oxidase RBOHD during plant immunity. *Plant Cell Physiol.* **56**, 1472–1480 (2015).
37. M. A. Torres, J. L. Dangl, J. D. Jones, *Arabidopsis* gp91phox homologues AtrbohD and AtrbohF are required for accumulation of reactive oxygen intermediates in the plant defense response. *Proc. Natl. Acad. Sci. U.S.A.* **99**, 517–522 (2002).
38. D. Chinchilla, Z. Bauer, M. Regenass, T. Boller, G. Felix, The *Arabidopsis* receptor kinase FLS2 binds flg22 and determines the specificity of flagellin perception. *Plant Cell* **18**, 465–476 (2006).
39. C. Zipfel *et al*., Perception of the bacterial PAMP EF-Tu by the receptor EFR restricts *Agrobacterium*-mediated transformation. *Cell* **125**, 749–760 (2006).
40. M. Roux *et al*., The *Arabidopsis* leucine-rich repeat receptor-like kinases BAK1/SERK3 and BKK1/SERK4 are required for innate immunity to hemibiotrophic and biotrophic pathogens. *Plant Cell* **23**, 2440–2455 (2011).
41. L. Li *et al*., The FLS2-associated kinase BIK1 directly phosphorylates the NADPH oxidase RbohD to control plant immunity. *Cell Host Microbe* **15**, 329–338 (2014).
42. A. Miya *et al*., CERK1, a LysM receptor kinase, is essential for chitin elicitor signaling in *Arabidopsis*. *Proc. Natl. Acad. Sci. U.S.A.* **104**, 19613–19618 (2007).
43. W. Zhang *et al*., *Arabidopsis* receptor-like protein30 and receptor-like kinase suppressor of BIR1-1/EVERSHED mediate innate immunity to necrotrophic fungi. *Plant Cell* **25**, 4227–4241 (2013).
44. J. Choi *et al*., Identification of a plant receptor for extracellular ATP. *Science* **343**, 290–294 (2014).
45. S. Ranf *et al*., A lectin S-domain receptor kinase mediates lipopolysaccharide sensing in *Arabidopsis thaliana*. *Nat. Immunol.* **16**, 426–433 (2015).
46. W. P. Luzuriaga-Loaiza *et al*., Synthetic rhamnolipid bolaforms trigger an innate immune response in *Arabidopsis thaliana*. *Sci. Rep.* **8**, 8534 (2018).
47. K. Shang-Guan *et al*., Lipopolysaccharides trigger two successive bursts of reactive oxygen species at distinct cellular locations. *Plant Physiol.* **176**, 2543–2556 (2018).
48. X. F. Xin, S. Y. He, *Pseudomonas syringae* pv. *tomato* DC3000: A model pathogen for probing disease susceptibility and hormone signaling in plants. *Annu. Rev. Phytopathol.* **51**, 473–498 (2013).
49. S. G. Costa, E. Déziel, F. Lépine, Characterization of rhamnolipid production by *Burkholderia glumae*. *Lett. Appl. Microbiol.* **53**, 620–627 (2011).
50. J. H. Ham, R. A. Melanson, M. C. Rush, *Burkholderia glumae*: Next major pathogen of rice? *Mol. Plant Pathol.* **12**, 329–339 (2011).

51. A. B. Stephan, H. H. Kunz, E. Yang, J. I. Schroeder, Rapid hyperosmotic-induced Ca^{2+} responses in *Arabidopsis thaliana* exhibit sensory potentiation and involvement of plastidial KEA transporters. *Proc. Natl. Acad. Sci. U.S.A.* **113**, E5242–E5249 (2016).
52. T. Lenarčič *et al*., Eudicot plant-specific sphingolipids determine host selectivity of microbial NLP cytolysins. *Science* **358**, 1431–1434 (2017).
53. N. C. Caiazza, R. M. Shanks, G. A. O'Toole, Rhamnolipids modulate swarming motility patterns of *Pseudomonas aeruginosa*. *J. Bacteriol.* **187**, 7351–7361 (2005).
54. A. Nickzad, F. Lépine, E. Déziel, Quorum sensing controls swarming motility of *Burkholderia glumae* through regulation of rhamnolipids. *PLoS One* **10**, e0128509 (2015).
55. X. Yu *et al*., Transcriptional responses of *Pseudomonas syringae* to growth in epiphytic versus apoplastic leaf sites. *Proc. Natl. Acad. Sci. U.S.A.* **110**, E425–E434 (2013).
56. M. E. Davey, N. C. Caiazza, G. A. O'Toole, Rhamnolipid surfactant production affects biofilm architecture in *Pseudomonas aeruginosa* PAO1. *J. Bacteriol.* **185**, 1027–1036 (2003).
57. H. Hirai *et al*., Glycosylation regulates specific induction of rice immune responses by *Acidovorax avenae* flagellin. *J. Biol. Chem.* **286**, 25519–25530 (2011).
58. F. Taguchi *et al*., Glycosylation of flagellin from *Pseudomonas syringae* pv. tabaci 6605 contributes to evasion of host tobacco plant surveillance system. *Physiol. Mol. Plant Pathol.* **74**, 11–17 (2009).
59. A. Hanuszkiewicz *et al*., Identification of the flagellin glycosylation system in *Burkholderia cenocepacia* and the contribution of glycosylated flagellin to evasion of human innate immune responses. *J. Biol. Chem.* **289**, 19231–19244 (2014).
60. G. Henry, M. Deleu, E. Jourdan, P. Thonart, M. Ongena, The bacterial lipopeptide surfactin targets the lipid fraction of the plant plasma membrane to trigger immune-related defence responses. *Cell. Microbiol.* **13**, 1824–1837 (2011).
61. M. N. Nasir *et al*., Differential interaction of synthetic glycolipids with biomimetic plasma membrane lipids correlates with the plant biological response. *Langmuir* **33**, 9979–9987 (2017).
62. M. Robineau *et al*., Synthetic mono-rhamnolipids display direct antifungal effects and trigger an innate immune response in tomato against *Botrytis cinerea*. *Molecules* **25**, 3108 (2020).
63. H. Abbasi, K. A. Noghabi, A. Ortiz, Interaction of a bacterial monorhamnolipid secreted by *Pseudomonas aeruginosa* MA01 with phosphatidylcholine model membranes. *Chem. Phys. Lipids* **165**, 745–752 (2012).
64. F. J. Aranda *et al*., Thermodynamics of the interaction of a dirhamnolipid biosurfactant secreted by *Pseudomonas aeruginosa* with phospholipid membranes. *Langmuir* **23**, 2700–2705 (2007).
65. A. Ortiz, F. J. Aranda, J. A. Teruel, Interaction of dirhamnolipid biosurfactants with phospholipid membranes: A molecular level study. *Adv. Exp. Med. Biol.* **672**, 42–53 (2010).
66. M. Sánchez, F. J. Aranda, J. A. Teruel, A. Ortiz, Interaction of a bacterial dirhamnolipid with phosphatidylcholine membranes: A biophysical study. *Chem. Phys. Lipids* **161**, 51–55 (2009).
67. N. Monnier *et al*., Exploring the dual interaction of natural rhamnolipids with plant and fungal biomimetic plasma membranes through biophysical studies. *Int. J. Mol. Sci.* **20**, 1009 (2019).
68. F. Lépine, E. Déziel, S. Milot, R. Villemur, Liquid chromatographic/mass spectrometric detection of the 3-(3-hydroxyalkanoyloxy) alkanoic acid precursors of rhamnolipids in *Pseudomonas aeruginosa* cultures. *J. Mass Spectrom.* **37**, 41–46 (2002).
69. R. Kownatzki, B. Tümmler, G. Döring, Rhamnolipid of *Pseudomonas aeruginosa* in sputum of cystic fibrosis patients. *Lancet* **1**, 1026–1027 (1987).
70. R. C. Read *et al*., Effect of *Pseudomonas aeruginosa* rhamnolipids on mucociliary transport and ciliary beating. *J. Appl. Physiol. (1985)* **72**, 2271–2277 (1992).
71. M. Somerville *et al*., Release of mucus glycoconjugates by *Pseudomonas aeruginosa* rhamnolipid into feline trachea *in vivo* and human bronchus *in vitro*. *Am. J. Respir. Cell Mol. Biol.* **6**, 116–122 (1992).
72. A. Germer *et al*., Exploiting the natural diversity of RhlA acyltransferases for the synthesis of the rhamnolipid precursor 3-(3-Hydroxyalkanoyloxy)alkanoic acid. *Appl. Environ. Microbiol.* **86**, e02317–e02319 (2020).
73. S. Ranf, Immune sensing of lipopolysaccharide in plants and animals: Same but different. *PLoS Pathog.* **12**, e1005596 (2016).
74. S. Compant, J. Nowak, T. Coenye, C. Clément, E. Ait Barka, Diversity and occurrence of *Burkholderia* spp. in the natural environment. *FEMS Microbiol. Rev.* **32**, 607–626 (2008).
75. E. Kay, F. Bertolla, T. M. Vogel, P. Simonet, Opportunistic colonization of *Ralstonia solanacearum*-infected plants by *Acinetobacter* sp. and its natural competence development. *Microb. Ecol.* **43**, 291–297 (2002).
76. M. W. Silby, C. Winstanley, S. A. Godfrey, S. B. Levy, R. W. Jackson, *Pseudomonas* genomes: Diverse and adaptable. *FEMS Microbiol. Rev.* **35**, 652–680 (2011).
77. I. K. Toth, L. Pritchard, P. R. J. Birch, Comparative genomics reveals what makes an enterobacterial plant pathogen. *Annu. Rev. Phytopathol.* **44**, 305–336 (2006).
78. X. Yu *et al*., Transcriptional analysis of the global regulatory networks active in *Pseudomonas syringae* during leaf colonization. *mBio* **5**, e01683–e14 (2014).
79. K. Zhu, C. O. Rock, RhlA converts beta-hydroxyacyl-acyl carrier protein intermediates in fatty acid synthesis to the beta-hydroxydecanoyl-beta-hydroxydecanoate component of rhamnolipids in *Pseudomonas aeruginosa*. *J. Bacteriol.* **190**, 3147–3154 (2008).
80. P. Buscaill *et al*., Glycosidase and glycan polymorphism control hydrolytic release of immunogenic flagellin peptides. *Science* **364**, eaav0748 (2019).
81. F. Taguchi *et al*., Effects of glycosylation on swimming ability and flagellar polymorphic transformation in *Pseudomonas syringae* pv. *tabaci* 6605. *J. Bacteriol.* **190**, 764–768 (2008).
82. J. M. Smith, A. Heese, Rapid bioassay to measure early reactive oxygen species production in *Arabidopsis* leave tissue in response to living *Pseudomonas syringae*. *Plant Methods* **10**, 6 (2014).
83. M. Magnin-Robert *et al*., Modifications of sphingolipid content affect tolerance to hemibiotrophic and necrotrophic pathogens by modulating plant defense responses in *Arabidopsis*. *Plant Physiol.* **169**, 2255–2274 (2015).
84. L.-J. Shu *et al*., Low cost, medium throughput depletion-binding assay for screening S-domain-receptor ligand interactions using in planta protein expression. *bioRxiv* [Preprint] (2021). https://doi.org/10.1101/2021.06.16.448648 (Accessed 18 June 2021).
85. S. König *et al*., *Arabidopsis* mutants of sphingolipid fatty acid α-hydroxylases accumulate ceramides and salicylates. *New Phytol.* **196**, 1086–1097 (2012).